HHS Public Access

Author manuscript

Chem Commun (Camb). Author manuscript; available in PMC 2017 September 14.

Published in final edited form as:

Chem Commun (Camb). 2013 September 25; 49(74): 8256–8258. doi:10.1039/c3cc44048f.

Highly luminescent, fluorinated semiconducting polymer dots for cellular imaging and analysis†

Yong Zhang, **Jiangbo Yu**, **Maria Elena Gallina**, **Wei Sun**, **Yu Rong**, and **Daniel T. Chiu**

Department of Chemistry, University of Washington, Seattle, Washington, USA. Fax: +1 206 685 8665; Tel: +1 206 543 1655

Abstract

A highly fluorescent fluorinated semiconducting polymer dot (Pdot) with a quantum yield of up to 49% was developed. The fluorinated Pdot was eight times brighter in cell-labeling applications than its non-fluorinated counterpart, and was rod shaped rather than spherical.

Semiconducting polymer dots (Pdots) have attracted tremendous interest in biological imaging and sensing because of their unique characteristics, such as high brightness, tunable emission, stability against photobleaching, high photon-emission rates, and non-toxicity.[1–12] Pdots can be prepared using nanoprecipitation, which has proven to be an effective way to prepare small-sized Pdots for both *in vivo* and *in vitro* biological applications. A number of fluorescent semiconducting polymers, such as poly[(9,9-dioctylfluorenyl-2,7-diyl)-*alt*-1,4-benzo-(2,1,3)-thiadiazole] (PFBT) and poly(*p*-phenylene vinylene), have been successfully used to make Pdots for cellular imaging, bio-orthogonal labeling, and *in vivo* tumor targeting because they have good fluorescent properties.[1,13–20] These successful applications point to the potential of Pdots in biological applications.

Fluorous materials have recently drawn much attention because of their interesting properties in applications such as liquid crystals, polymer light-emitting diodes, and polymer photovoltaic cells.[21–24] Fluorine is a small atom that can be introduced onto polymer chains with minimal effect on steric hindrance. Highly fluorinated polymers can be dissolved in fluorous solvents, a feature that facilitates the purification and processing of the polymers. Fluorous polymers are also biocompatible.[24] Swager and coworkers reported that rigid perfluoroalkyl chains introduced onto a conjugated polymer can increase the polymer's quantum yield both in solution and in solid state compared with its non-fluorinated analogs.[24] Other groups have also demonstrated that the strong electron-withdrawing fluorine atom can enhance the photovoltaic performance of the polymer by lowering the energy levels and improving the $\pi - \pi$ stacking of conjugated polymers.[21–23] These results suggest that fluorous materials have great promise in tuning the material properties of conjugated polymers.

†Electronic supplementary information (ESI) available: Synthesis of monomers and polymers, experimental details and quantum yields. See DOI: 10.1039/c3cc44048f

Correspondence to: Daniel T. Chiu.

We decided to investigate the effect of attaching a fluorine atom onto a semiconducting polymer backbone to make a mono-fluorine-substituted benzothiadiazole-based polymer (PFDPFBT, Scheme 1). We found that the presence of a fluorine atom increased the quantum yield of the resulting Pdots by ~5× when compared to the non-fluorinated analog (PFDPBT). Furthermore, in cell-labelling applications, the fluorinated Pdot offered ~8× improvement in cell brightness over the non-fluorinated Pdots in flow cytometry applications. Cellular imaging studies also showed that these fluorinated Pdots were highly fluorescent and effective at specific cellular targeting without noticeable non-specific background labelling.

Scheme 1 shows the synthetic route of PFDPFBT and PFDPBT. The synthesis of monomers is shown in ESI.† The monomer **2** was synthesized in two steps from 5-fluoro-4,7-dibromo-[2,1,3]benzothiadiazole.[22] The Suzuki polymerization between **1** and **2** with the $Pd(PPh_3)_4$ catalyst gave the fluorinated PFDPFBT. Non-fluorinated PFDPBT was synthesized under the same conditions. Both polymers showed good solubility in the organic solvent THF. The number-average molecular weights (M_n) of PFDPFBT and PFDPBT estimated by gel permeation chromatography (GPC) were 24.5 and 19.8 kDa with a polydispersity index (PDI) of 1.8 and 2.1, respectively.

To form Pdots, we used the nanoprecipitation method, which we have previously described.[13–15] Briefly, we rapidly injected PFDPFBT (or PFDPBT) and PS-PEG-COOH (polystyrene-grafted ethylene oxide functionalized with carboxyl groups) dissolved in THF into water under ultrasonication (Fig. 1); PS-PEG-COOH has little effect on the molar absorption coefficient of PFDPFBT or PFDPBT. The Pdots formed by this method had the carboxylic acid groups on their surfaces, which were amenable for subsequent bioconjugation.

We studied the sizes and shapes of the Pdots by dynamic light scattering (DLS) and transmission electron microscopy (TEM). Fig. 2 shows the representative DLS and TEM images of PFDPFBT–PS-PEG-COOH and PFDPBT–PS-PEG-COOH Pdots at a ratio of 20:5 (semiconducting polymer: PS-PEG-COOH) in weight. From DLS data (Fig. 2a and c), both Pdots showed similar hydrodynamic diameters of ~16 nm, which is consistent with the TEM measurements. As measured by TEM, PFDPBT– PS-PEG-COOH Pdots were spherical particles with an average diameter of 14 nm (Fig. 2d). Surprisingly, we found that the fluorinated Pdots had rod or ellipsoidal shapes (Fig. 2b) when blended with PS-PEG-COOH. The aspect ratio was between 1.6 and 3, with a length between 20 and 40 nm. Recent studies have shown that F–H and/or F–F interactions can induce stronger packing in fluorinated polymers compared to their non-fluorinated analogs.[21,23] As a result, we believe that the formation of ellipsoidal Pdots may be caused by the interactions of F–H and/or F–F of PFDPFBT and PS-PEG-COOH, which then led to a more rigid and extended conjugated polymer backbone that was harder to fold onto itself during nanoparticle formation, resulting in rod-shaped Pdots.

†Electronic supplementary information (ESI) available: Synthesis of monomers and polymers, experimental details and quantum yields. See DOI: 10.1039/c3cc44048f

Fig. 3 shows the absorption and photoluminescence (PL) spectra of PFDPFBT–PS-PEG-COOH and PFDPBT–PS-PEG-COOH Pdots. The charge transfer (CT) absorption peak in the long wavelength region for PFDPBT–PS-PEG-COOH Pdot was at ~425 nm; the CT peak for the PFDPFBT–PS-PEG-COOH Pdot, with the introduction of a fluorine atom, blue-shifted to ~410 nm. This result suggests that the introduction of a fluorine atom enhanced CT between the donor (fluorene segment) and the acceptor (fluorobenzothiadiazole segment). The PL peak of the PFDPBT–PS-PEG-COOH Pdot was at ~530 nm; the PL peak was blue-shifted to ~510 nm, with a purer green emission, for PFDPFBT–PS-PEG-COOH Pdots. Bare PFDPFBT and PFDPBT Pdots without any PS-PEG-COOH showed similar quantum yields (QYs) of 25% and 28%, respectively, which indicates that the two types of polymer chains have a similar degree of aggregation in Pdots. We note that the QYs of PFDPBT and PFDPFBT in THF are 88% and 83%, respectively. However, the difference in quantum yields between the two types of Pdots when blended with PS-PEG-COOH displayed a remarkable difference: the quantum yield of PFDPFBT–PS-PEG-COOH (20:5 w/w) Pdots increased to 46% but that of PFDPBT–PS-PEG-COOH Pdots decreased to 7%. This large difference in QY caused by the presence of PS-PEG-COOH prompted us to study how the amount of blended PS-PEG-COOH affected the resulting QY of the two types of Pdots. The QY of PFDPFBT–PS-PEG-COOH Pdots exhibited a gradual increase when the weight ratio was increased from 20:1 to 20:10 (Fig. S1, ESI[†]). In contrast, for PFDPBT–PS-PEG-COOH Pdots, the QY first decreased to 7% at a ratio of 20:5 and then slightly increased from 7% to 10% at higher PS-PEG-COOH amounts.

To determine whether the effect of PS-PEG-COOH was caused by the hydrophobic polystyrene (PS) or the hydrophilic PEG-COOH, we prepared PFDPFBT (or PFDPBT) Pdots with pure PS. The PFDPFBT–PS and PFDPBT–PS Pdots showed a comparable QY (50% *vs.* 60%), which indicate that the hydro-philic group (PEG-COOH) in PS-PEG-COOH played the dominant role in causing the large QY difference between the different types of Pdots. For PFDPBT Pdots, the low QY may have been caused by PEG-COOH-induced aggregation quenching, in which PFDPBT chains aggregated or stacked more densely. In PFDPFBT–PS-PEG-COOH Pdots, F–F and/or F–H interactions, together with the strong hydrophobic properties of F atoms, may have led to a rigid and extended polymer chain, which minimized the aggregation-induced quenching. The rigid and extended polymer chain present in PFDPFBT–PS-PEG-COOH Pdots also had an impact on the shape of the resultant Pdots (Fig. 2b).

To evaluate the performance of the two types of Pdots for biological applications, we applied them to flow cytometry and cellular imaging. We conjugated the Pdots to streptavidin *via* the 1-ethyl-3-[3-dimethylaminopropyl]carbodiimide hydrochloride (EDC)-catalyzed coupling reaction (see experimental section for details). We then used them to label MCF-7 cells incubated with biotinylated antibodies against the cell-surface protein EpCAM. The MCF-7 cells were incubated with a biotinylated primary anti-EpCAM antibody and then with Pdot–streptavidin probes. Fig. 4a shows the flow cytometry results. There was excellent separation between Pdot–streptavidin-labeled cells and the negative control, which were cells incubated with Pdots but in the absence of the biotinylated primary antibody. MCF-7 cells labeled with bioconju-gated PFDPFBT–PS-PEG-COOH Pdots exhibited a much higher intensity than

cells labeled with bioconjugated PFDPBT–PS-PEG-COOH Pdots under identical labelling and experimental conditions. Quantitative analysis of the flow cytometry results obtained with a 510/50 nm bandpass and a 502 nm long-pass filter showed that the average fluorescence intensity of MCF-7 cells labeled with PFDPFBT–PS-PEG-COOH Pdots was ~8 times brighter than those labeled with PFDPBT–PS-PEG-COOH Pdots. This result is consistent with the QY and molar absorption coefficient of both Pdots. We also used a different band-pass filter (530 nm/30 nm) and obtained similar results (Fig. S2, ESI†).

We also studied the Pdot–streptavidin labelled MCF-7 cells with confocal fluorescence imaging (Fig. 4b and c). Again, we did not observe any noticeable non-specific background binding of the Pdots to the cell surface, where cells were incubated with Pdot–streptavidin but without biotinylated primary antibodies. The positive cells were bright and clearly visible. We repeated the experiment with 488 nm excitation (Fig. S3, ESI†), a commonly used wavelength in bioimaging and flow cytometry, and observed similarly bright cells with no detectable non-specific binding of the Pdots to the cells.

In conclusion, we successfully developed a novel fluorescent fluorinated semiconducting polymer, PFDPFBT. The Pdots were prepared by the nanoprecipitation method. TEM measurements revealed that most of the nanoparticle shapes of PFDPFBT–PS-PEG-COOH Pdots were ellipsoid or rod, instead of the spherical shapes seen for PFDPBT–PS-PEG-COOH Pdots. PFDPFBT–PS-PEG-COOH Pdots have a QY as high as 49%, but the QY of PFDPBT–PS-PEG-COOH Pdots is only around 6–10%. Flow cytometry experiments showed that the fluorescence intensities of MCF-7 cancer cells labeled with PFDPFBT–PS-PEG-COOH–streptavidin Pdot probes were eight times higher compared to those labeled with PFDPBT–PS-PEG-COOH–strep-tavidin Pdot probes. Fluorescent cell images with both types of Pdots targeted to a cell-surface marker on MCF-7 cells showed specific subcellular labelling. The data indicate that the introduction of a fluorine atom onto the polymer backbone makes a significant difference in the physical and biological properties of Pdots, as seen with PFDPFBT–PS-PEG-COOH Pdots, making them promising probes for biological detection.

We thank the Keck Imaging Center and the Center of Nanotechnology at the University of Washington for the use of their facilities. This work was supported by the Department of Defense CDMRP Program (BC100510), the Life Science Discovery Fund, the National Institutes of Health (GM GM085485), and the University of Washington.

Supplementary Material

Refer to Web version on PubMed Central for supplementary material.

Notes and references

1. Wu C, Chiu DT. Angew Chem, Int Ed. 2013; 52:3086.
2. Wu C, Bull B, Szymanski C, Christensen K, McNeill J. ACS Nano. 2008; 2:2415. [PubMed: 19206410]
3. Schutze F, Stempfle B, Jungst C, Woll D, Zumbusch A, Mecking S. Chem Commun. 2012; 48:2104.
4. Li K, Liu B. J Mater Chem. 2012; 22:1257.

5. Li K, Ding D, Huo D, Pu KY, Ngo NPT, Hu Y, Li Z, Liu B. Adv Funct Mater. 2012; 22:3107.
6. Petkau K, Kaeser A, Fischer I, Brunsveld L, Schenning APHJ. J Am Chem Soc. 2011; 133:17063. [PubMed: 21913650]
7. Tuncel D, Demir HV. Nanoscale. 2010; 2:484. [PubMed: 20644748]
8. Pecher J, Mecking S. Chem Rev. 2010; 110:6260. [PubMed: 20684570]
9. Howes P, Green M, Levitt J, Suhling K, Hughes M. J Am Chem Soc. 2010; 132:3989. [PubMed: 20175539]
10. Yu J, Wu C, Sahu SP, Fernando LP, Szymanski C, McNeill J. J Am Chem Soc. 2009; 131:18410. [PubMed: 20028148]
11. Kim S, Lim CK, Na J, Lee YD, Kim K, Choi K, Leary JF, Kwon IC. Chem Commun. 2010; 46:1617.
12. Feng X, Yang G, Liu L, Lv F, Yang Q, Wang S, Zhu D. Adv Mater. 2012; 24:637. [PubMed: 21932281]
13. Wu C, Hansen SJ, Hou Q, Yu J, Zeigler M, Jin Y, Burnham DR, McNeill JD, Olson JM, Chiu DT. Angew Chem, Int Ed. 2011; 50:3430.
14. Wu C, Jin Y, Schneider T, Burnham DR, Smith PB, Chiu DT. Angew Chem, Int Ed. 2010; 49:9436.
15. Wu C, Schneider T, Zeigler M, Yu J, Schiro PG, Burnham DR, McNeill JD, Chiu DT. J Am Chem Soc. 2010; 132:15410. [PubMed: 20929226]
16. Rong Y, Wu C, Yu J, Zhang X, Ye F, Zeigler M, Gallina ME, Wu IC, Zhang Y, Chan YH, Sun W, Uvdal K, Chiu DT. ACS Nano. 2013; 7:376. [PubMed: 23282278]
17. Zhang X, Yu J, Wu C, Jin Y, Rong Y, Ye F, Chiu DT. ACS Nano. 2012; 6:5429. [PubMed: 22607220]
18. Yu J, Wu C, Zhang X, Ye F, Gallina ME, Rong Y, Wu IC, Sun W, Chan YH, Chiu DT. Adv Mater. 2012; 24:3498. [PubMed: 22684783]
19. Ye F, Wu C, Jin Y, Wang M, Chan YH, Yu J, Sun W, Hayden S, Chiu DT. Chem Commun. 2012; 48:1778.
20. Chan YH, Wu C, Ye F, Jin Y, Smith PB, Chiu DT. Anal Chem. 2011; 83:1448. [PubMed: 21244093]
21. Price SC, Stuart AC, Yang LQ, Zhou HX, You W. J Am Chem Soc. 2011; 133:4625. [PubMed: 21375339]
22. Zhang Y, Chien SC, Chen KS, Yip HL, Sun Y, Davies JA, Chen FC, Jen AKY. Chem Commun. 2011; 47:11026.
23. Zhang Y, Zou JY, Cheuh CC, Yip HL, Jen AKY. Macromolecules. 2012; 45:5427.
24. Lim J, Swager TM. Angew Chem, Int Ed. 2010; 49:7486.

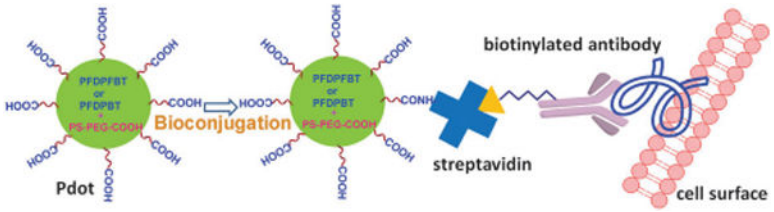

Fig. 1.

Illustration of PFDPFBT–PS-PEG-COOH and PFDPBT–PS-PEG-COOH Pdots and their bioconjugated probes for cellular imaging.

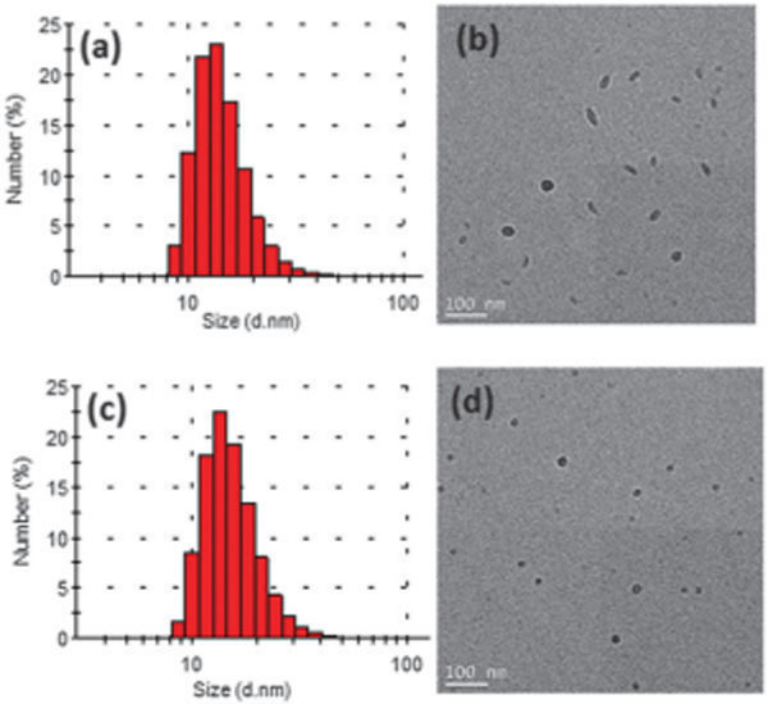

Fig. 2.

The hydrodynamic diameter measured by dynamic light scattering and TEM images of (a and b) PFDPFBT–PS-PEG-COOH Pdots and (c and d) PFDPBT–PS-PEG-COOH Pdots.

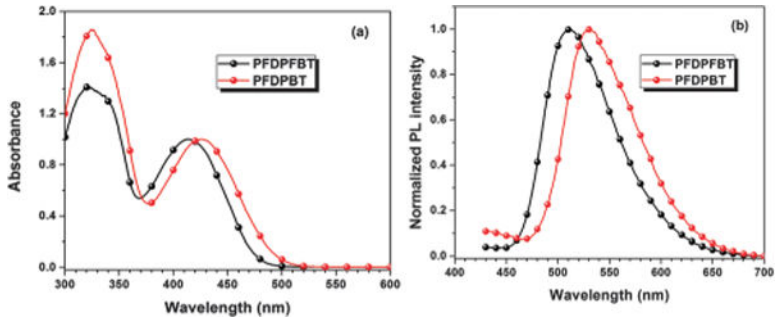

Fig. 3.

The UV-Vis and PL spectra of PFDPFBT–PS-PEG-COOH Pdots and PFDPBT– PS-PEG-COOH Pdots in water.

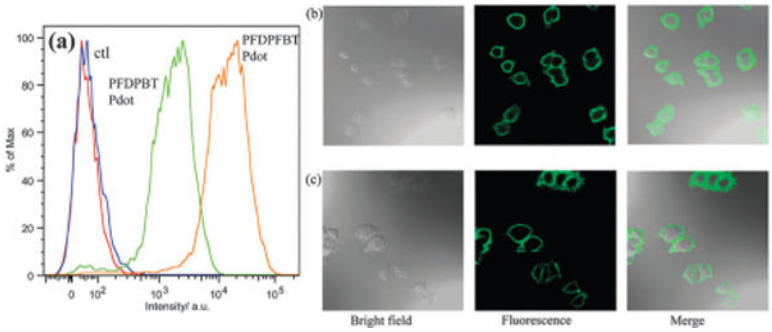

Fig. 4.

(a) Flow cytometry of MCF-7 breast cancer cells labeled *via* non-specific binding (negative control) and positive specific targeting (positive labeling) using PFDPFBT–PS-PEG-COOH and PFDPBT–PS-PEG-COOH Pdot bioconjugates. Confocal fluorescence images of MCF-7 breast cancer cells labeled with a PFDPFBT–PS-PEG-COOH–streptavidin Pdot probe (b) and a PFDPBT–PS-PEG-COOH–streptavidin Pdot probe (c).

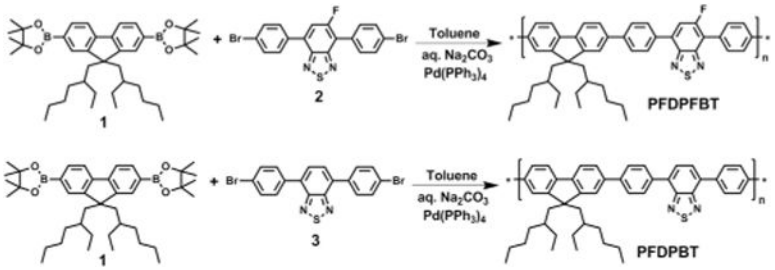

Scheme 1.
Synthetic route toward polymers.